AUT Journal of Civil Engineering

AUT J. Civil Eng., 4(3) (2020) 289-302
DOI: 10.22060/ajce.2019.16045.5562

Energy-Based Method for Evaluating Cracks and Resistance of Fiber Reinforced Ultra-High Strength Concrete under Impact Loads

M. Aziminezhad[1], S. Mardi[2], AR. Shourestani[2], P. Hajikarimi[3,*], F. Moghadas Nejad[3]

[1]Department of Civil Engineering, Imam Khomeini International University, Qazvin, Iran
[2]Department of Civil Engineering, Qazvin Branch, Islamic Azad University, Qazvin, Iran
[3]Department of Civil & Environmental Engineering, Amirkabir University of Technology, Tehran, Iran

ABSTRACT: In order to adjust the lack of sufficient ductility of ultra-high strength concrete (UHSC), different types of fiber were used in this study. This research investigates the effect of glass, polypropylene and steel fibers on the impact resistance and crack propagation of fiber reinforced UHSCs by implementing slab specimens with a dimension of 300×300×30 mm. The experimental program includes 18 specimens with 1%, 1.5% and 2% of concrete volume for each type of fiber which was made with two different mixing methods (Ordinary fiber reinforced concrete (FRC) and high performance fiber reinforced concrete (HPFRC)). In this study, specimens were placed under a low-velocity impact loading (5.42 m/s) within a fixed rigid constrained setup. The health index and the crack propagation correlation are two criteria for determining the trend of degradation and impact resistance reduction. Results demonstrate that the FRCs show higher impact resistance in comparison with the HPFRC because the HPFRC method doesn't provide enough cohesion between concrete and fibers. The obtained results also show that FRC specimens include polypropylene, endure higher impact resistance with a greater amount of health index rather than other specimens. By increasing the fiber's volume in the specimens fabricated with glass and polypropylene, a more homogenous composite was formed and energy spread more uniform over all faces of FRC specimen.

Review History:

Received: 2019-03-24
Revised: 2019-08-15
Accepted: 2019-08-17
Available Online: 2019-08-25

Keywords:

UHSC
Fiber reinforced concrete
Impact resistance
Crack propagation

1- INTRODUCTION

The use of high strength and ultra-high strength concrete (UHSC) has been rising in recent decades. Large-scale projects and high-rise buildings lead to more demands for concretes with higher strength than ordinary ones. The definition of the UHSC is changing every few years based on ongoing advances in the field of concrete technology and it varies depending on the geographical basis [1]. Some researchers have been suggested a specific limit for defining the UHSC. El-Dieb [2], Courtial and his coworkers [3] suggested that concretes with higher strength than 100 MPa could be classified as the UHSC.

The UHSCs reinforced with fibers are considered as reliable composite materials with enhanced stability, ductility and high energy absorption capacity. Various types of fiber are available with different behavior such as steel fibers [4], polypropylene [5], glass [6] and etc. The UHSC behaves in a brittle and explosive manner during the failure process. Therefore, it is necessary to use the above-mentioned fibers to gain desired performance. A proper curing condition is essential to fabricate the ultra-high strength concrete. Among the available curing methods, autoclave and thermal curing are suggested to achieve the best results [7, 8].

From safety point of view, it is necessary to provide ample protection for concrete elements against external hazards such as unexpected blast, extrinsic impact and so on. The concrete resistance against such impacts indicates durability and quality of materials as well as its implementation efficacious. Some researches focused on the ability of concrete to absorb energy before its failure as a major factor [9, 10]. The impact resistance is defined as the ability of concrete to withstand sudden shock applied for a short time step. Several experimental programs were carried out to investigate the effect of impact on concretes reinforced with fibers.

The concrete slabs reinforced with carbon fiber reinforced polymer (CFRP) showed greater ultimate bearing capacity in comparison with ordinary slabs. Ong et al. [11] showed that the type of fibers and its volume are related to the impact resistance of a FRC. Polyolefin, polyvinyl alcohol, and hooked-end steel fibers were studied with a variation of 1 and 2% of concrete volume. The results showed that steel fibers reduce crack propagation and increase energy absorption in comparison with other fibers. Polyvinyl alcohol fiber's slabs also showed higher energy absorption compared to polyolefin fibers. The usage of higher volume of fibers resulted in better performance and higher energy absorption in all specimens.

Rao et al. [12] investigated behavior of slurry-infiltrated fibrous concrete (SIFCON) under applied impact loading. It was reported that SIFCON slabs showed better performance

*Corresponding author's email: pouria.hajikarimi@gmail.com

under impact loading in comparison with fiber-reinforced, reinforced cement concrete (RCC) and plain cement concrete (PCC) slabs. Generally, split tensile, ultimate impact, and compressive strengths of SIFCON concrete increased by adding higher fiber volume. A study on the UHSC under repeated impact loading with various steel fiber volumes were investigated by Tai and Wang [13]. It was distinguished that strain hardening rate and damage softening effect have significant influences on the deterioration progress under dynamic loading. In specimens with a lower content of steel fibers, more micro-cracks appeared to extend along the weakest band which resulted in speeding up the failure. Sovjak et al. [14] reported that the UHSC reinforced with higher fiber volume performs better against impact loadings. The specimen without fibers got multiple macro-cracks in first blows and splintered into pieces. Almusallam et al. [5] reported that hybrid fibers decrease the area of damage in slabs under impact loading and slow the process of crack propagation. It also reduces the mass ejection of concrete from samples. The Geometrical attributes of fibers have more effects on the slabs reinforced with hybrid fibers than their material properties. Mao et al. [15] conducted an investigation on the UHSC slabs reinforced with fibers under blast loading. It was shown that the way fibers orient and distribute directly influence on the slab's behavior.

The Support type and layout significantly influence on concrete slabs' behavior. These two parameters were studied by Anil et al. [16] under a low-velocity impact loading. The number of blows, damaged area, and crack propagation pattern were recorded for comparison. It was reported that the number of blows for specimens with fixed supports are higher than those with hinge ones. In specimens with fixed supports, cracks started from the middle of the slab and spread toward supports with the larger distribution area. For hinge supports, cracks mostly propagated in the middle area of specimens.

Radnic et al. [17] investigated the behavior of ordinary reinforced concrete (RC) slabs and RC slabs reinforced with strips of CFRP which are applied on its external surface. The impact test was performed with different height on both types of above-mentioned specimens. The repeated impact tests showed that the stiffness of slabs decreases on each impact and the value of stiffness reduction is higher for greater drop heights.

Yu et al. [18] investigated energy absorption capacity of the UHSC reinforced with different types of steel fiber. It was indicated that the use of hybrid steel fibers enhances the mechanical properties of concrete, However, the usage of steel fibers with hooked-ends were suggested to improve energy absorption capacity in quasi-static mode. The UHSC reinforced with hybrid fibers have shown more energy absorption capacity compared to hooked-ends steel fibers under projectile impact loading. An identical experience was reported for less scabbing on the rear surface.

In this paper, the performance of the UHSC slabs including impact resistance and crack propagation under low-velocity impact loading was studied. The specimens were cast by using two mixing methods: high performance fiber reinforced concrete (HPFRC) and ordinary fiber reinforced concrete (FRC). Each method contains 9 specimens, including glass, polypropylene, and steel fibers with 1, 1.5 and 2% of concrete volume for each type of fiber. One slab was cast without fiber as the control specimen. The effect of adding fibers on the number of impacts, crack patterns, and slab deterioration after each impact was investigated. The health index was introduced as a new index for determining slabs' condition by considering the number of impacts and undamaged area of each surface. The root mean square (RMSE) method was used to study the correlation of crack propagation on top and bottom surface of the slabs for all impact steps up to failure. At the final stage, the preferable mixing method and the fiber type with optimum usage volume were determined to achieve the best performance against low-velocity impact loads.

In this paper, materials, mixture design, sample preparation and impact test methods are introduced. Then, results and discussion are presented and analyzed qualitatively by considering number of drops to failure and quantitatively by defining the health index. Finally, summary and concluding remarks are presented.

2- MATERIALS AND TEST METHODS

2-1- Materials

The commercial ASTM C150 [19] Portland cement type II provided by Jovin Khorasan™ and silica fume as a pozzolanic additive were used in this study. Their chemical analysis shows in Table 1. Polycarboxylate ether superplasticizer with the specific gravity of 1080 kg/m^3 was used to reduce water-cement ratio and increase the compressive strength. The grading diagram of quartezit aggregates (micro-sand) acquired from

Table 1. Chemical composition of cement and silica fume

Cement (%)	Silica fume (%)
20.38	93.6
4.13	1.3
3.82	0.9
62.96	0.5
3.5	1
2.87	0.1
0.98	_

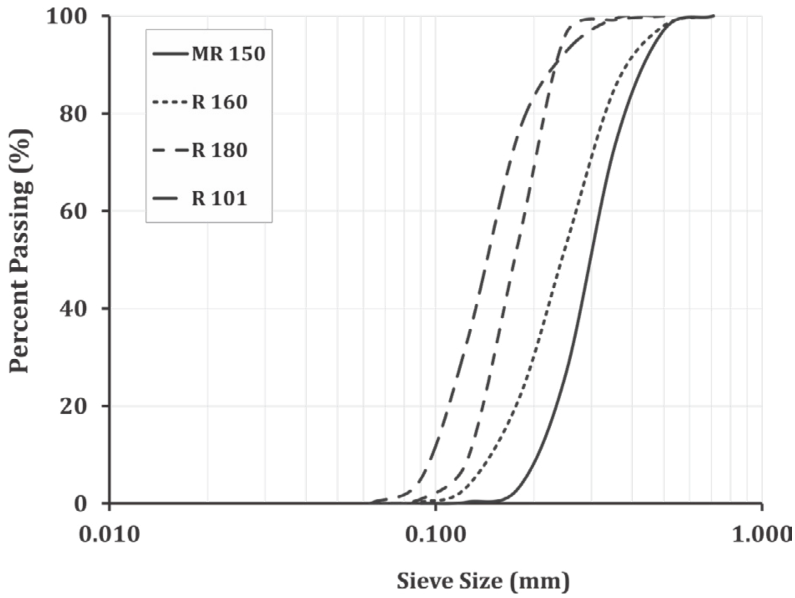

Fig. 1. Grading diagram of quartezit aggregates

Table 2. Specification of steel, polypropylene and glass fibers

Fiber type	Length (mm)	Diameter (μm)	Shape	Specific gravity (g/cm^3)	Tensile strength (MPa)	Modulus of elasticity (GPa)
Steel (st)	50	800	Hooked-ends	7.8	1400	200
Polypropylene (pp)	12	19	Crimped	0.91	450	5
Glass (g)	12	17	Plain	2.58	3445	72.3

Iran Kansar™ which was used in this research program depicts in Fig. 1 with their commercial codes including MR 150, R 160, R 180 and R 101. In addition, ZS 200 powder (another product of Iran Kansar) was used as filler with a size smaller than 75 microns. The water absorption of MR 150, R 160, R 180, R 101 and ZS 200 is 4, 8.4, 7.2, 13 and 30%, respectively. Additionally, steel, polypropylene, and glass are three kinds of fibers used in this study which their physical and mechanical properties are listed in Table 2. Fig. 2 shows the diameter of fibers. A scanning electron microscope (SEM) was used to measure the diameter of polypropylene and glass fibers.

2-2- Mixture Design

In this research, four different amounts of binders are considered for making the UHSC including 750, 940, 1100 and 1300 kg/m^3. The water-cement ratio was considered to be 0.18 for all mixtures. The total water for fabricating each sample was determined based on the water absorption of the aggregates plus the required water for the mixture. A constant ratio of cement-silica fume (80/20) and an averagely 2.5% of superplasticizer (by weight of binder materials) and various aggregate blends (based on Fig. 1) were designed to obtain an appropriate UHSC. These mix types can be seen in Fig. 3 regarding the amount of their binder. Moreover, the flowability of concrete was measured by mini-slump flow and 100×100×100mm cubic samples tested for compressive strength respectively according to EFNARC [20] and BS 1881-116 [21]. These results are presented in Fig. 4. The 1100c4 was chosen as the optimized mixture design in terms of compressive strength, the weight of binder materials and workability.

2-3- Sample Preparation

The Concrete mix was prepared with three kinds of fibers separately in different contents including 1, 1.5, and 2% of concrete volume. Two types of mixing procedure were designed for casting concrete specimens: high performance fiber reinforced concrete (HPFRC) and fiber reinforced concrete (FRC). For FRC, a dry mixing of cement, silica fume, and aggregates were performed for 2 minutes and then water and super-plasticizer were gradually added to the mix during 1 minute. The process of mixing water and super-plasticizer was held on for 5 minutes and finally followed by adding fibers which were mixed for 2 minutes. A 300×300×30 mm slab molds were filled by vibrating for average one minute. The high performance fiber reinforced concrete (HPFRC) is

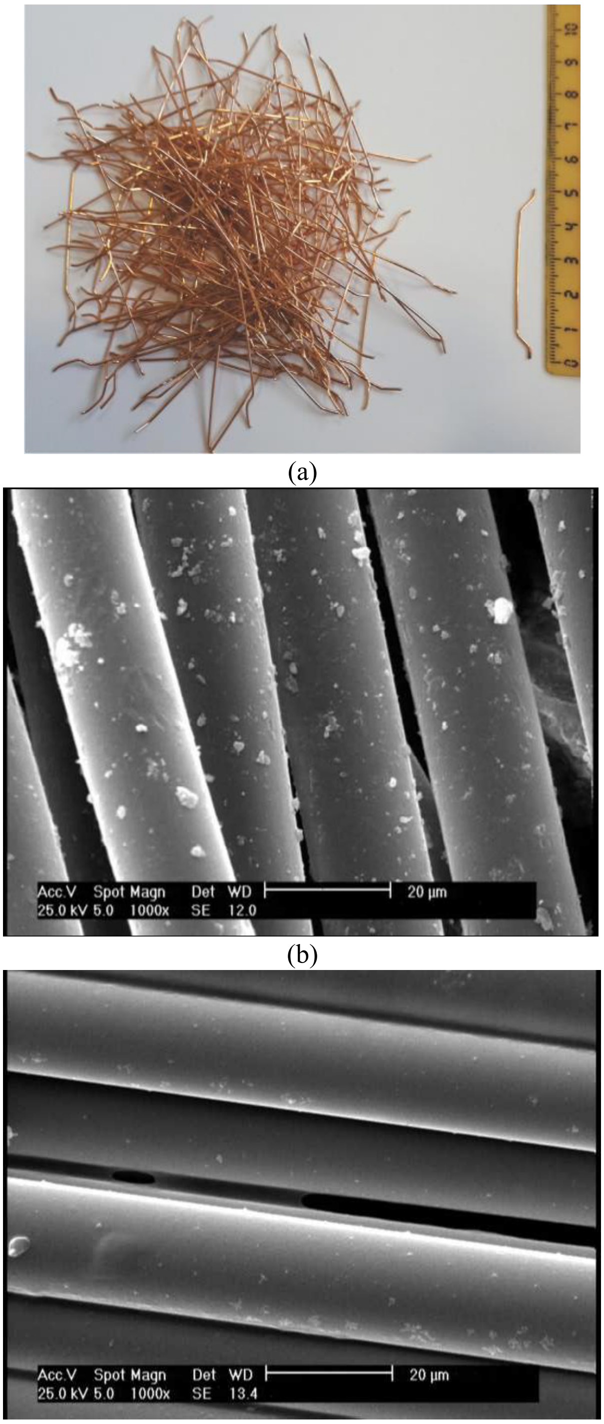

Fig. 2. Snapshots of (a) steel, (b) polypropylene and (c) glass fibers

made based on an innovative method called SIFCON [22, 23]. In this method, after making concrete using a similar procedure as FRC, concrete was poured to the slab mold in three layers with a height of 1 cm for each layer using a short vibration of average 10 sec.

Consequently, the fabricated slabs contained 5 layers including top concrete layer, upper fiber layer (1 cm below the top surface of the slab), middle concrete layer, lower fiber layer (1 cm above the bottom surface of the slab) and bottom concrete layer. The specimens were kept in moist condition for the first 24 hours. In order to reach the final strength of concrete, specimens were put in thermal curing water for 4 days at the temperature of 60°C. All specimens were made based on 1100c4 mixture design.

2-4- Impact Test

In this study, the impact test contained a steel cylinder weighed 8.5 kg, 50 mm diameter and 550 mm height dropped from 1.5 m height to impact the sample with final velocity of 5.42 m/s at the impact moment. The slab specimen was placed in a fixed setup. In order to avoid stress concentration between the specimen and supports, a rubber strip was used to fix the specimen at all rounds. Fig. 5 illustrates the impact test setup and details of constraints. After each impact test, cracks in the top and bottom face of the slab were marked and a photograph was recorded to investigate crack propagation patterns in the specimen.

3- RESULTS AND DISCUSSION

As a simple and rough result of the designed impact test, Fig. 6 shows the number of impacts for causing failure versus fiber content of the UHSC including FRC and HPFRCs, respectively. For fiber reinforced concrete, it can be seen that samples with PP fibers can resist against the greater amount of impacts in comparison with samples containing steel and glass fibers. For 2% of PP, the number of 39 impacts were recorded which is so significant among all FRC samples. Based on Fig. 6-a, it is evident that by increasing the amount of fiber content, the impact resistance of FRC specimens enhances for all types of fiber.

Regarding to Fig. 6-b, it can be concluded that increasing the amount of steel fiber had no significant effect on the impact resistance of HPFRCs. It seems that steel layer could not form a compound with concrete and the impact resistance can be just related to the strength of steel fibers for selected contents. For samples reinforced by glass fibers, it can be seen that increasing the amount of fibers led to decreasing the impact resistance of HPFRC which simply can be explained. Therefore, by increasing the amount of glass fiber content and forming an individual layer of these fibers, the impact resistance of specimens decreases. Actually, in the procedure of making HPFRCs especially for the greater amount of fibers, it is not possible to form an integrated composite of fibers and concrete. Also, the 1.5% of PP fibers is an optimized content for forming a compound of concrete and fibers in order to resist against impact. According to Fig. 6 and comparing between results of FRC and HPFRCs, it can be seen that FRC has better performance rather than HPFRC.

By considering patterns of crack propagation in the FRC specimens, there are some interesting results discussed in the following. Fig. 7 shows patterns of crack propagation for FRC samples at their top and bottom surfaces reinforced using 2% of each fiber which shows the best impact resistance according to Fig. 6-a. As it can be seen in this Figure, for samples reinforced by steel fibers, a concentrated failure took place at the top face and a disruption at the bottom face while for glass and PP samples, a distribution of cracks can be clearly seen.

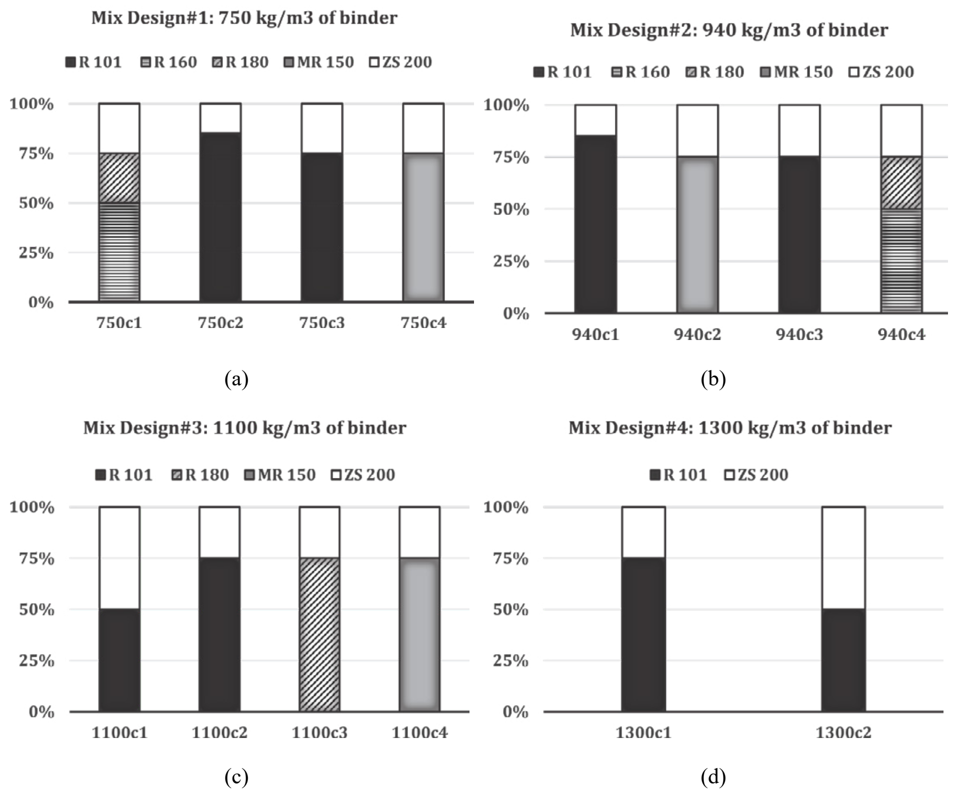

Fig. 3. Mixture design of all UHSC samples with (a) 750, (b) 940, (c) 1100 and (d) 1300 kg/m^3 of binder

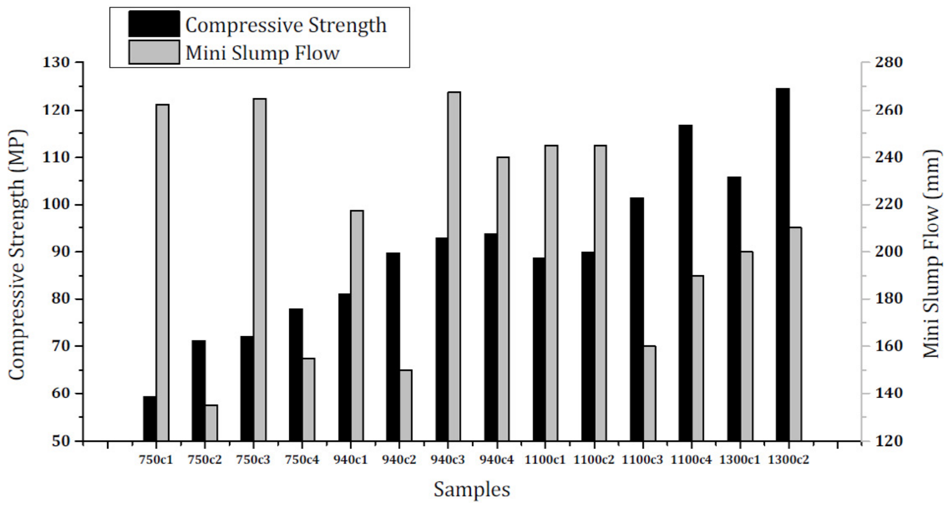

Fig. 4. Results of compressive strength and mini slump flow of all UHSC concrete

Fig. 8 shows such pattern similar to Fig. 7 for all HPFRC samples. This Figure depicts the top and bottom face of HPFRC for fiber content which had the greatest amount of impact resistance based on Fig. 6-b led to 2% of steel, 1.5% of PP and 1% of glass fiber. A similar pattern as FRC can be considered for HPFRC demonstrates that PP and glass can distribute impact energy on the top face of samples while samples containing steel fibers just transmitted the energy to the bottom face.

The major change in crack patterns is the way cracks distribute over slab area in front and rear face. It can be seen that while in specimens with steel fibers, the upper face was almost untouched and there was no significant track of cracks, the rear surface of the slab was heavily damaged when specimen reached failure. This is identical for both mixture methods. By contrast, it can be seen that specimens with PP or glass fiber, had experienced damage and crack propagated even on their front surface which shows the ability of fiber to use larger area of slab to dissipate the applied impact and that is one of reasons why they could generally endure more

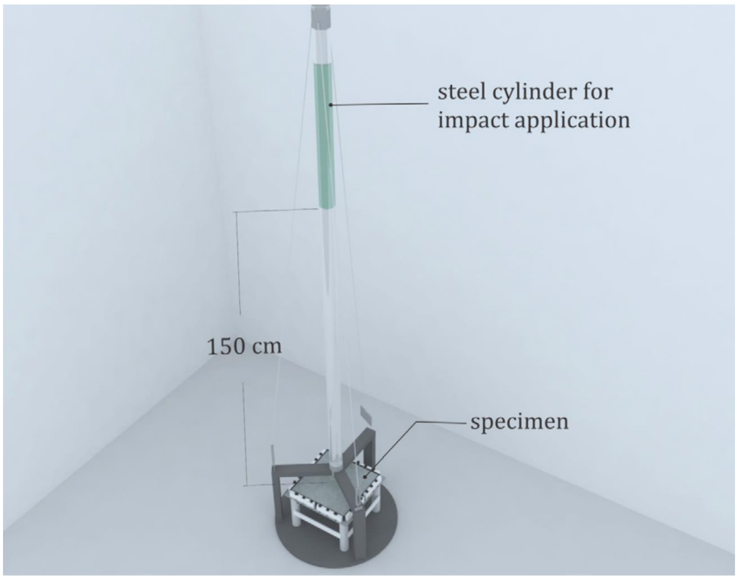

(a)

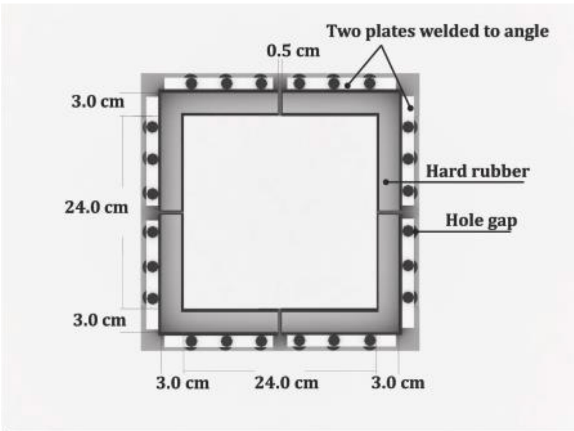

(b)

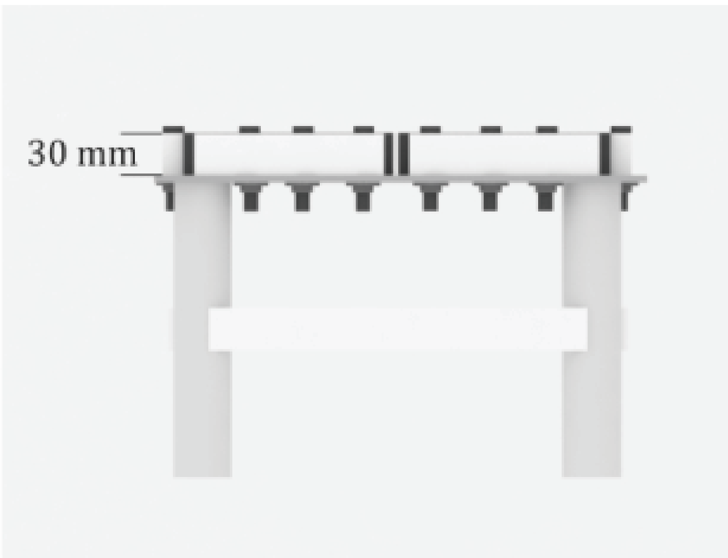

(c)

Fig. 5. Impact test setup and details of constraints including (a) isometric, (b) plan and (c) section view of setup

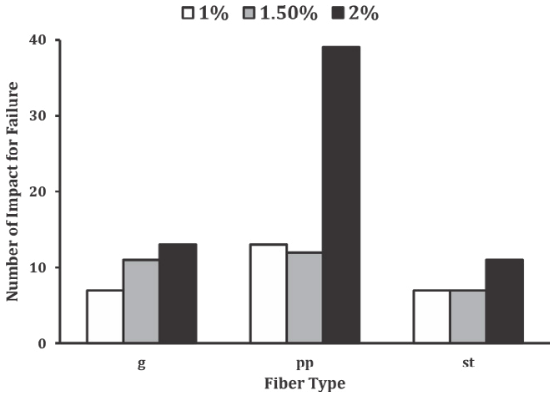

(a)

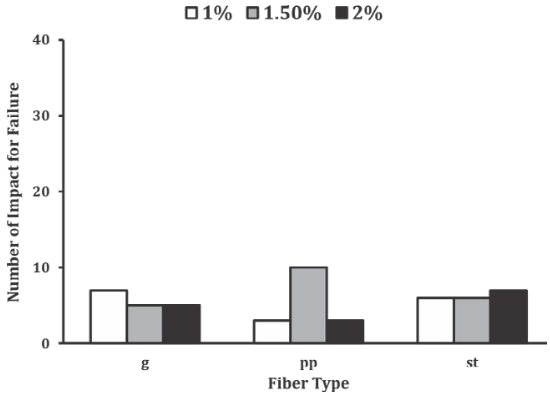

(b)

Fig. 6. Number of Impacts for failure versus fiber type for (a) FRC and (b) HPFRCs

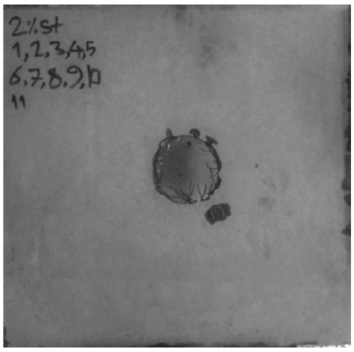

(a)

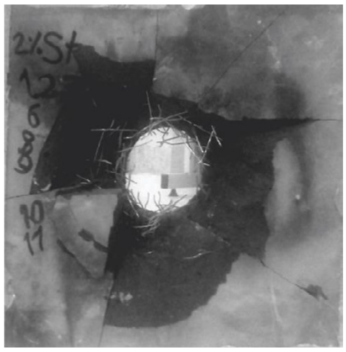

(b)

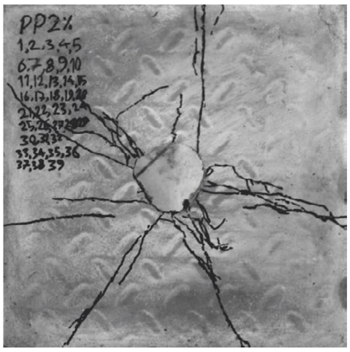

(c)

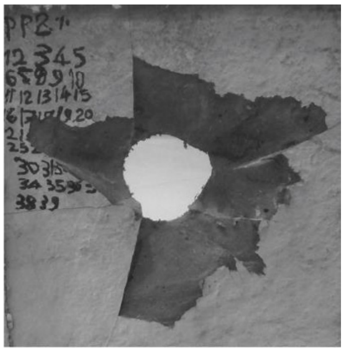

(d)

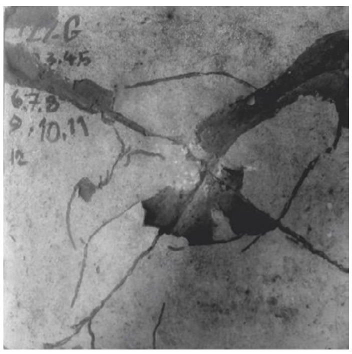

(e)

(f)

Fig. 7. Crack propagation patterns of FRC fiber reinforced specimens of (a) top and (b) bottom face of steel fiber, (c) top and (d) bottom face of PP, (e) top and (f) bottom face of glass fiber samples

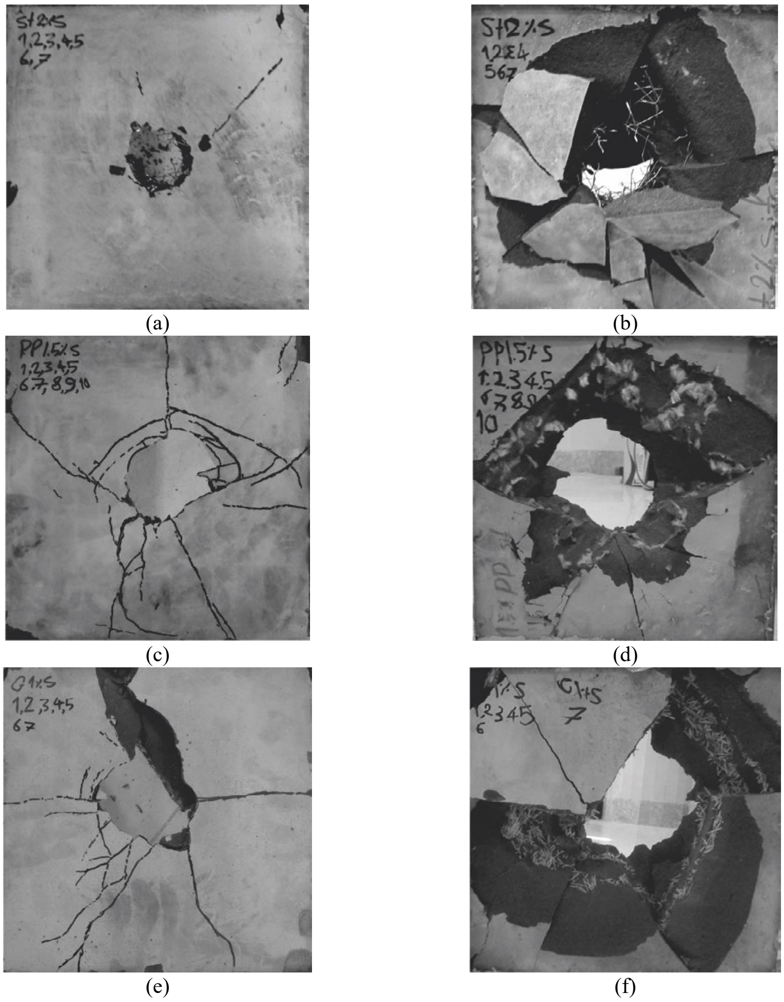

Fig. 8. Crack propagation patterns of HPFRC samples of (a) top and (b) bottom face of samples with 2% of steel fiber, (c) top and (d) bottom face of samples with 1.5% of PP, (e) top and (f) bottom face of samples with 1% of glass fiber

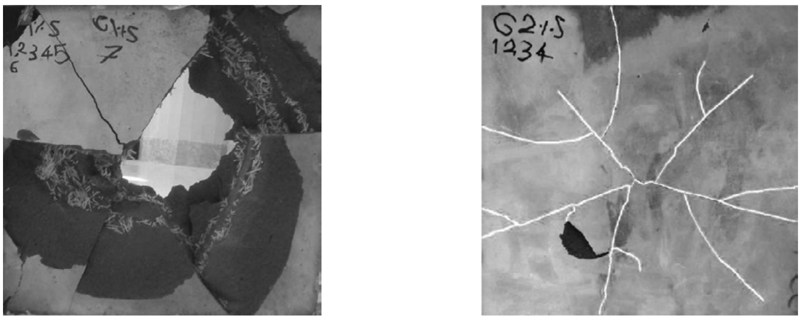

(a) (b)

Fig. 9. A sample for determining (a) damaged area and (b) total crack length

number of impacts before reaching failure.

In order to quantify results of impact test and going into more depth, the value of the damaged area and total crack length of the top and bottom surface of all FRC and HPFRC specimens is measured at each impact step up to failure. The damaged area can be an index for determining the impact resistance reduction after each drop. Also, the crack length is an appropriate parameter for evaluating energy distribution over surface and thickness of fiber reinforced UHSC slabs. A simple code was developed implementing image processing of MATLAB for determining the damaged area and the crack length.

Fig. 9 depicts the procedure of this determination in which a polygon specifies the perimeter of the damaged area and also crack edges are highlighted with a different color.

Fig. 10 illustrates the percentage of the intact area which is

Table 3. Result of top face intact area for all FRC and HPFRC samples

Specimen type	HPFRC Intact Area (%)	FRC Intact Area (%)
g1%	88.64	94.15
g1.5%	95.06	91.25
g2%	96.75	71.07
pp1%	96.52	94.64
pp1.5%	91.99	94.13
pp2%	97.19	96.67
st1%	96.7	95.7
st1.5%	94	92.24
st2%	95.64	96.22

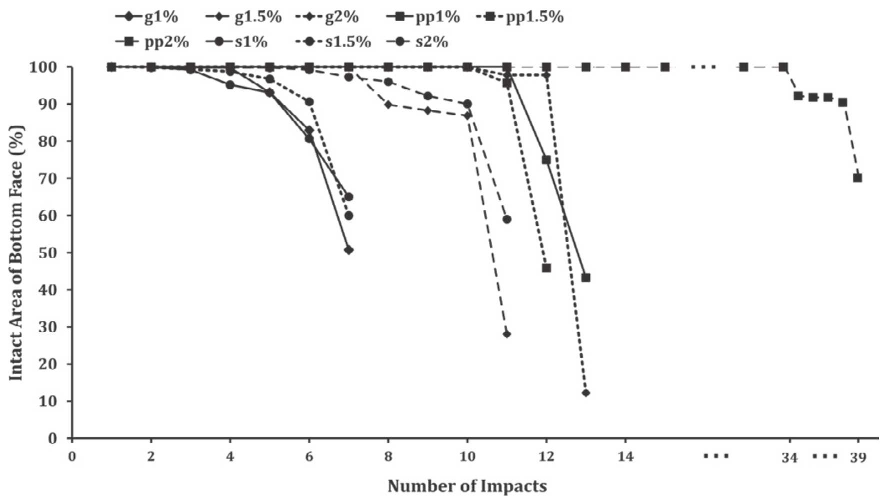

(a)

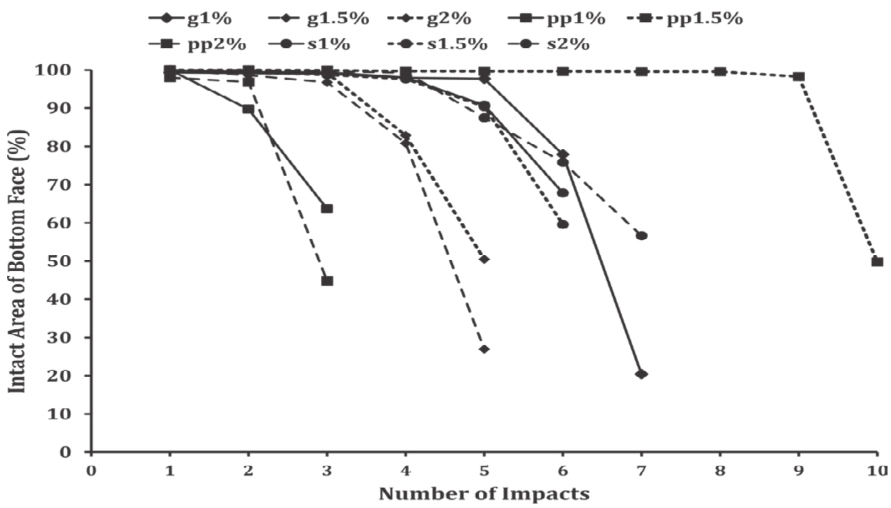

(b)

Fig. 10. The percentage of intact area for all samples of (a) FRC and (b) HPFRC

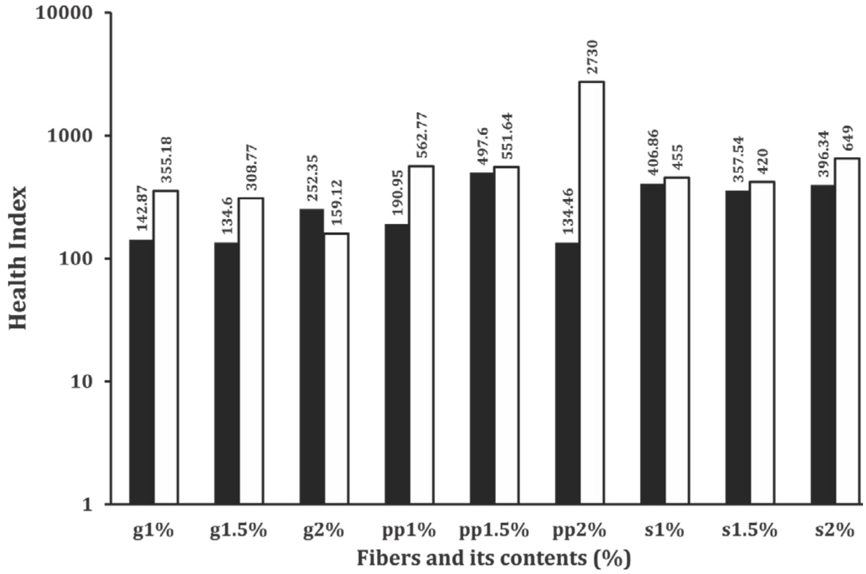

Fig. 11. Health index of all fibers for both FRC and HPFRC

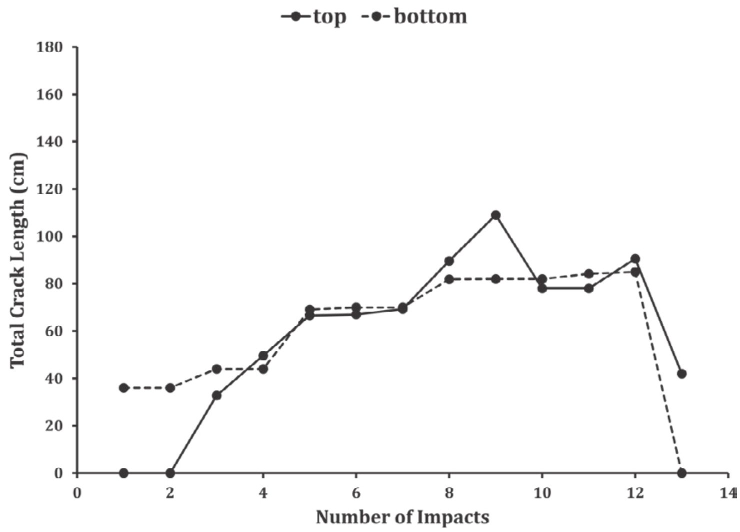

(a)

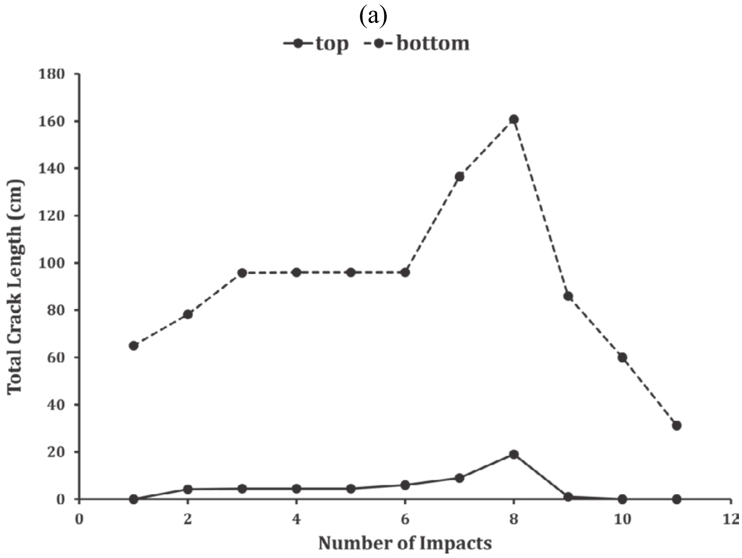

(b)

Fig. 12. Crack length of top and bottom face of FRC samples with (a) g2% and (b) st2%

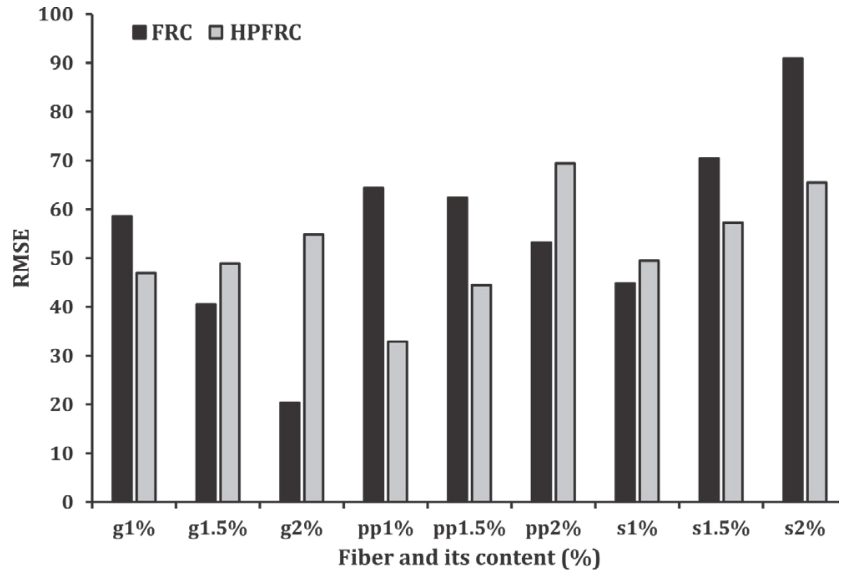

Fig. 13. RMSE value for both FRC and HPFRC

measured for just the bottom face of each sample during the impact test. The percentage of the intact area is determined based on Eq. (1):

$$\text{intact area}\left(\%\right)=100-\left(\frac{\text{damaged area}}{\text{initial intact area}}\times 100\right) \tag{1}$$

Similar to the bottom face, the percentage of the damaged area was also determined for the top face but observation shows that there is no considerable difference between this data for the top surface of all samples and cannot make a sense to evaluate the effect of fibers on their impact resistance and can be eliminated. Table 3 shows the percentage of the intact area after the final drop for the top face of all samples calculated based on Eq. (1).

Based on Fig. 10, a slighter trend of deterioration can be seen for HPFRC in comparison with FRC. However, it is not possible to judge only based on this Figure and it is required to define a specific parameter to compare FRC and HPFRC specimens with different percentages of fibers. Therefore, the health index (HI) is defined as percentage of intact area for the last drop multiplied by total number of drops.

Regarding to definition of HI, it is obvious that a higher amount of this index is more desirable. This parameter can make an appropriate balance between the effect of total number of drops and percentage of the intact area. As the input values are concerned, number of drops ranged from 7 to 39 for FRC and 3 to 11 for HPFRC specimens. This domain for intact area of surfaces ranged from 71.07 to 96.67 and from 88.64 to 97.19 percent of total slab area for FRC and HPFRC specimens, respectively. Fig. 11 depicts the health index for both FRC and HPFRC. For an instance, g2% for FRC can endure the greatest amount of drops between glass samples based on Fig. 6-a while it has the lowest amount of HI in comparison with other glass fiber reinforced specimens. It shows that although g2% withstand against more drops but simultaneously its deterioration is higher than other samples.

As it can be seen in Fig. 11, pp2% of FRC has higher HI and pp2% of HPFRC has lower one. g1%, st2%, and pp2% are the best alternatives for FRC and g2%, st1% and pp1.5% are the best ones for HPFRC due to its greatest amount of the HI. For glass fibers, g1% of FRC and HPFRC both endure 7 drops to failure but regarding lower damaged area of FRC, it has better performance than HPFRC one. It can be explained by considering the deterioration process. The g1% sample in FRC mix formed a better compound with concrete compared to HPFRC g1% sample. After the last drop that caused highest damage and total collapse of the slab (which is not desirable due to safety specifications), the lower HI is obtained. It means that not only numbers of drops are vital but it is also essential to have a higher intact area in order to provide post-impact rehabilitation in elements of structures. It can be seen in both FRC and HPFRC that st1.5% with more volume of steel fibers than st1% led to lower HI despite having the same number of drops in both methods. Although adding extra steel fiber caused reduction of intact area in st2%, steel fibers could resist more impacts for FRC and demonstrated better total performance for st2% according to the health index.

For investigating energy spread based on crack propagation, crack length was recorded after each drop on the top and bottom surface until failure. In order to determine the ability of concrete and different fibers' compounds for evaluating energy expansion, the root mean square error (RMSE) method was used to find a correlation between the crack length of the top and bottom surfaces for both FRC and HPFRC. The lower value of RMSE shows the better fiber performance for determining the correlation between the top and bottom face's cracks. The RMSE equation is defined as follows:

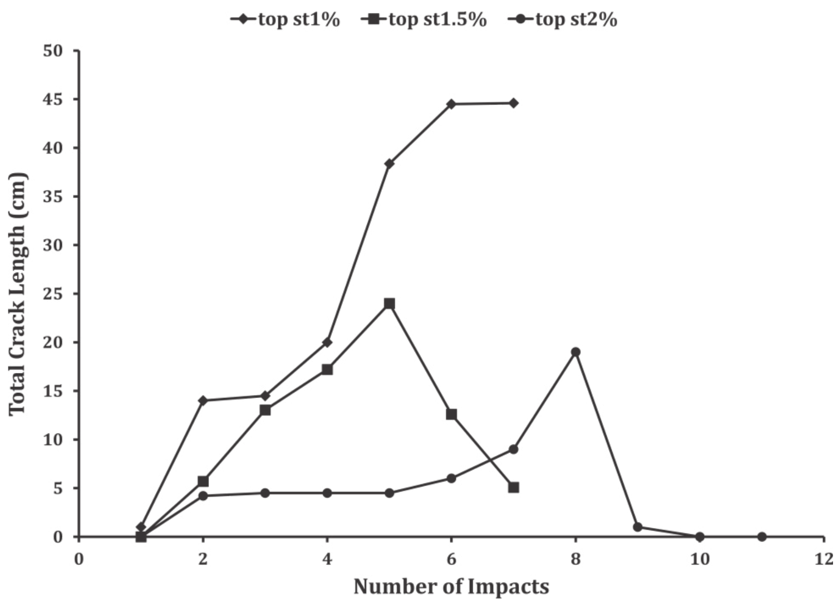

(a)

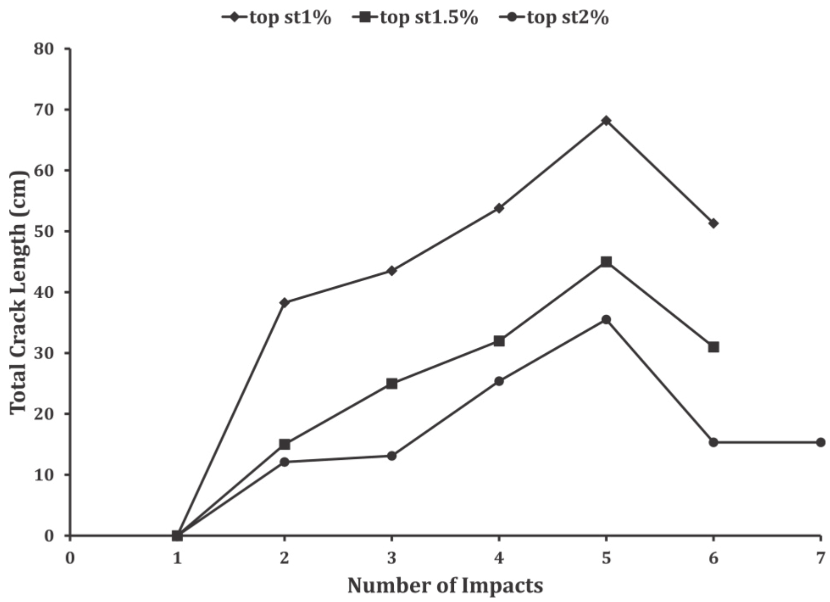

(b)

Fig. 14. Total crack length of top face of steel fiber reinforced samples for (a) FRC and (b) HPFRC

$$RMSE = \sqrt{\frac{\sum_{t=1}^{n}\left(L_{bottom,t} - L_{top,t}\right)^2}{n}} \tag{3}$$

where L_{bottom} is the total crack length of the bottom surface; L_{top} is the total crack length of top surface and n is number of total drops. For instance, Fig. 12 shows diagram of crack length and drop number for g2% and st2% of FRC specimens in each impact step for the top and bottom surfaces. The output data of the above-mentioned diagram allows calculating RMSE value. Fig. 12-a shows that there is less difference between the crack length of the top and bottom surface for g2%. Therefore, the RMSE value will be least. On the other hand, Fig. 12-b shows a major difference between the top and bottom diagrams so the RMSE value will be much higher.

Fig. 13 depicts RMSE value for all specimens. For Glass and polypropylene fibers in the FRC method, by increasing the fibers' volume, the RMSE value decreases which shows more correlation between cracks of the top and bottom surfaces. It can be easily explained that by increasing the fiber volume, the more homogenous composite is formed and energy spreads more uniform due to each impact over all faces of the specimen. For the steel fiber in both FRC and HPFRC, increasing the fiber volume results in less correlation between the top and bottom surface's cracks. There is no change in steel fiber shape during mix in the FRC method while glass and polypropylene fibers lose their initial shape and fully integrate with concrete. This results that steel fibers only have different direction within concrete without losing initial shape and make clumps (especially for higher volumes) which is very similar to HPFRC mix method. It has been found that increasing steel fiber results in more local energy absorption by steel fibers so it results in less correlation (more RMSE value) between cracks of the top and bottom surface. Based on Fig. 14, it is also visible that crack length decreases in the top surface by increasing the steel fiber volume which approves the local energy absorption of steel fibers.

As impact force was applied on slab specimen, PP and glass fibers prevent to discrete concrete components by forming a semi-continuous randomize distributed complex grid of fibers, hence the impact force distributed all over faces of the specimen and cracks appear on top and bottom of slab surfaces. However, steel fibers prevent to discrete by a sparse grid of fibers. Therefore, spalling pieces of concrete in these specimens were larger than PP and glass ones and less continuity was observed for force transferring. Increasing the glass and polypropylene fiber volume in HPFRC method indicates that there is less correlation between top and bottom surface (similar to steel fibers) and it results in a higher RMSE value. It is known that HPFRC method doesn't provide enough cohesion between concrete and fibers.

4- CONCLUSION

In this research, an energy-based approach is used for evaluating crack propagation and resistance of fiber reinforced UHSC under low-velocity impact loads. Two different methods for making fiber reinforced UHSC is implemented including ordinary fiber reinforced concrete (FRC) and high performance fiber reinforced concrete (HPFRC) which are well-known methods in the literature. Three different fibers containing glass, polypropylene, and steel are used to reinforce UHSC concrete with three percentages of 1, 1.5 and 2% of concrete volume. By measuring damaged area and crack length of each slab sample, two new indices are used to evaluate the effect of fiber and its content on low-velocity impact resistance of each fiber reinforced UHSC. According to the experimental results, it is evident that mechanical behavior of fiber reinforced concretes fabricated with different casting methods is not identical and the type of fiber used significantly influenced on the impact load resistance of FRC and HPFRC slab specimens. Based on qualitative and quantitative analysis of the experimental results, the following conclusions can be obtained:

§ The impact resistance of FRC enhances for all types of fiber by increasing the amount of fiber content.

§ FRC has better performance rather than HPFRC in terms of number of impacts for failure.

§ pp2% of FRC has the highest HI and pp2% of HPFRC has the lowest one. g1%, st2%, and pp2% are the best alternatives for FRC and g2%, st1% and pp1.5% are the best ones for HPFRC due to its greatest amount of the HI.

§ By increasing the fiber volume in glass and pp samples, a more homogenous composite is formed and energy spreads more uniform due to each impact over all faces of FRC specimen.

§ The HPFRC method doesn't provide enough cohesion between concrete and fibers.

ACKNOWLEDGMENT

This research was supported by the Construction and Concrete Research Center of Qazvin Islamic Azad University.

REFERENCES

[1] ACI Committee 363, Report on High-Strength Concrete, American Concrete Institute, Farmington Hills, MI, (2010).

[2] A.S. El-Dieb, Mechanical, durability and microstructural characteristics of ultra-high-strength self-compacting concrete incorporating steel fibers, Materials & Design, 30(10) (2009) 4286-4292.

[3] M. Courtial, M.N. de Noirfontaine, F. Dunstetter, M. Signes-Frehel, P. Mounanga, K. Cherkaoui, A. Khelidj, Effect of polycarboxylate and crushed quartz in UHPC: Microstructural investigation, Construction and Building Materials, 44 (2013) 699-705.

[4] A.A. Shah, Y. Ribakov, Recent trends in steel fibered high-strength concrete, Materials & Design, 32(8) (2011) 4122-4151.

[5] T.H. Almusallam, A.A. Abadel, Y.A. Al-Salloum, N.A. Siddiqui, H. Abbas, Effectiveness of hybrid-fibers in improving the impact resistance of RC slabs, International Journal of Impact Engineering, 81 (2015) 61-73.

[6] M.E. Arslan, Effects of basalt and glass chopped fibers addition on fracture energy and mechanical properties of ordinary concrete: CMOD measurement, Construction and Building Materials, 114 (2016) 383-391.

[7] D. Mostofinejad, M.R. Nikoo, S.A. Hosseini, Determination of optimized mix design and curing conditions of reactive powder concrete (RPC), Construction and Building Materials, 123 (2016) 754-767.

[8] S. Nie, S. Hu, F. Wang, P. Yuan, Y. Zhu, J. Ye, Y. Liu, Internal curing – A suitable method for improving the performance of heat-cured concrete, Construction and Building Materials, 122 (2016) 294-301.

[9] S.H. Park, D.J. Kim, S.W. Kim, Investigating the impact resistance of ultra-high-performance fiber-reinforced concrete using an improved strain energy impact test machine, Construction and Building Materials, 125 (2016) 145-159.

[10] [9] K. Onoue, H. Tamai, H. Suseno, Shock-absorbing capability of lightweight concrete utilizing volcanic pumice aggregate, Construction and Building Materials, 83 (2015) 261-274.

[11] K.C.G. Ong, M. Basheerkhan, P. Paramasivam, Resistance of fibre concrete slabs to low velocity projectile impact, Cement and Concrete Composites, 21(5) (1999) 391-401.

[12] H.S. Rao, V.G. Ghorpade, N.V. Ramana, K. Gnaneswar, Response of SIFCON two-way slabs under impact loading, International Journal of Impact Engineering, 37(4) (2010) 452-458.

[13] Y.-S. Tai, I.-T. Wang, Elucidating the mechanical behavior of ultra-high-strength concrete under repeated impact loading, Structural engineering & mechanics, 37(1) (2011) 1-15.

[14] [13] R. Sovják, T. Vavřiník, P. Máca, J. Zatloukal, P. Konvalinka, Y. Song, Experimental Investigation of Ultra-high Performance Fiber Reinforced Concrete Slabs Subjected to Deformable Projectile Impact, Procedia Engineering, 65 (2013) 120-125.

[15] [14] L. Mao, S.J. Barnett, A. Tyas, J. Warren, G.K. Schleyer, S.S. Zaini, Response of small scale ultra high performance fibre reinforced concrete slabs to blast loading, Construction and Building Materials, 93 (2015) 822-830.

[16] Ö. Anil, E. Kantar, M.C. Yilmaz, Low velocity impact behavior of RC slabs with different support types, Construction and Building Materials, 93 (2015) 1078-1088.

[17] J. Radnić, D. Matešan, N. Grgić, G. Baloević, Impact testing of RC slabs strengthened with CFRP strips, Composite Structures, 121 (2015) 90-103.

[18] R. Yu, P. Spiesz, H.J.H. Brouwers, Energy absorption capacity of a sustainable Ultra-High Performance Fibre Reinforced Concrete (UHPFRC) in quasi-static mode and under high velocity projectile impact, Cement and Concrete Composites, 68 (2016) 109-122.
[19] ASTM C150 / C150M-20, Standard Specification for Portland Cement, ASTM International, West Conshohocken, PA, (2020), www.astm.org
[20] EFNARC, Specification and guidelines for self-compacting concrete, Association House, Surrey, UK, (2002).
[21] BS 1881-116, Method for determination of compressive strength of concrete cubes, (2003).
[22] A.E. Naaman, D. Otter, H. Najm, Elastic modulus of SIFCON in tension and compression, Materials Journal, 88(6) (1992) 603-613.
[23] Y. Farnam, S. Mohammadi, M. Shekarchi, Experimental and numerical investigations of low velocity impact behavior of high-performance fiber-reinforced cement based composite, International Journal of Impact Engineering, 37(2) (2010) 220-229.

HOW TO CITE THIS ARTICLE

M. Aziminezhad, S. Mardi, AR. Shourestani, P Hajikarimi, F. Moghadas Nejad, Energy-Based Method for Evaluating Cracks and Resistance of Fiber Reinforced Ultra-High Strength Concrete under Impact Loads, AUT J. Civil Eng., 4(3) (2020) 289-302.

DOI: 10.22060/ajce.2019.16045.5562